

# Chaotic universe in the $z = 2$ Hořava-Lifshitz gravity

Yun Soo Myung,<sup>1,\*</sup> Yong-Wan Kim,<sup>1,†</sup> Woo-Sik Son,<sup>2,‡</sup> and Young-Jai Park<sup>2,§</sup>

<sup>1</sup>*Institute of Basic Science and School of Computer Aided Science, Inje University, Gimhae 621-749, Korea*

<sup>2</sup>*Department of Physics and WCU-SSME Program Division, Sogang University, Seoul 121-742, Korea*

The deformed  $z = 2$  Hořava-Lifshitz gravity with coupling constant  $\omega$  leads to a nonrelativistic “mixmaster” cosmological model. The potential of theory is given by the sum of IR and UV potentials in the ADM Hamiltonian formalism. It turns out that adding the UV-potential cannot suppress chaotic behaviors existing in the IR-potential.

PACS numbers: 98.80.Qc, 98.80.Bp, 04.60.Pp, 98.80.Jk

Keywords: Hořava-Lifshitz gravity, quantum gravity, mixmaster universe

## I. INTRODUCTION

Recently, quantum gravity at a Lifshitz point, which is power-counting renormalizable and hence potentially UV complete, was proposed by Hořava [1–3]. This theory, unlike string theory, is not intended to be a unified theory but quantum gravity. Specific cosmological implications of  $z = 3$  Hořava-Lifshitz gravity with the Friedmann-Robertson-Walker metric based on isotropy and homogeneity have recently been shown in [4–6], including homogeneous vacuum solution with chiral primordial gravitational waves [7] and nonsingular cosmological evolution with the big bang of standard and inflationary universe replaced by a matter bounce [8–10]. As far as the cosmological solutions are concerned, there is no difference between  $z = 2$  [1] and  $z = 3$  [2] Hořava-Lifshitz gravities because the Cotton tensor vanishes when using the Friedmann-Robertson-Walker metric. Furthermore, one has introduced the deformed  $z = 3$  Hořava-Lifshitz gravity to find asymptotically flat background [11, 12].

On the other hand, the equations of general relativity lead to singularities when we look at the equations backwards the origin of time. Especially, we concentrate on a temporal singularity of the solutions to the Einstein equations for the mixmaster model (Bianchi IX Universe) describing an anisotropic and homogeneous cosmology. It was well known that the approach to singularity shows a chaotic behavior. The mixmaster universe [13–20] could be described by a Hamiltonian dynamical system in a 6D phase space. Belinsky, Khalatnikov, and Lifshitz (BKL) had conjectured that this 6D phase system could be well approximated by a 1D discrete Gauss map that is known to be chaotic as one approaches the singularity [21]. Chernoff and Barrow suggested that the mixmaster 6D phase space could be split into the product of a 4D phase space and a 2D phase space having regular variables [15]. Following Cornish and Levin [17], Lehner and Di Menza found that the chaos in the mixmaster

universe is obtained for the Hamiltonian system with potential having fixed walls, which describes the curvature anisotropy [19]. However, it turned out that the mixmaster chaos could be suppressed by (loop) quantum effects [22, 23].

Hence it is very interesting to investigate cosmological application of Hořava-Lifshitz gravity in conjunction with the mixmaster universe based on the anisotropy and homogeneity because the Hořava-Lifshitz gravity is a strong candidate for quantum gravity. However, we will not make any quantum operation on the Hořava-Lifshitz gravity. In this work, we will make a progress on this direction.

Getting an associated Hamiltonian within the ADM formalism [24] of deformed  $z = 2$  Hořava-Lifshitz gravity [1, 11, 25], we find two potentials in 6D phase space: IR-potential  $V_{IR}$  from 3D curvature  $R$  and UV-potential  $V_{UV}$  from curvature square terms of  $R^2$  and  $R_{ij}R^{ij}$  with UV coupling parameter  $\omega$ . In 4D phase space, we find that the UV-potential cannot suppress chaotic behaviors existing in the IR-potential. After an extended analysis with movable wall, the chaotic behaviors persist in the 6D phase space.

## II. DEFORMED $z = 2$ HOŘAVA-LIFSHITZ GRAVITY

The action of the deformed  $z = 2$  Hořava-Lifshitz gravity [1, 11] takes the form in the (1+3)D spacetimes

$$S_\lambda = \int dt d^3x \sqrt{g} N \left[ \frac{2}{\kappa^2} (K_{ij} K^{ij} - \lambda K^2) + \mu^3 R + \frac{\kappa^2 \mu^2 (1 - 4\lambda)}{32(1 - 3\lambda)} R^2 - \frac{\kappa^2 \mu^2}{8} R_{ij} R^{ij} \right] \quad (1)$$

with three parameters  $\kappa$ ,  $\mu$ , and  $\lambda$ . In the case of  $\lambda = 1$ , the above action leads to

$$S_{\lambda=1} = \int dt d^3x \sqrt{g} N \left[ \frac{2}{\kappa^2} (K_{ij} K^{ij} - K^2) + \mu^3 \left( R - \frac{2}{\omega} (R_{ij} R^{ij} - \frac{3}{8} R^2) \right) \right] \quad (2)$$

\*Electronic address: ysmmyung@inje.ac.kr

†Electronic address: ywkim65@gmail.com

‡Electronic address: dawnmail@sogang.ac.kr

§Electronic address: yjpark@sogang.ac.kr

where the UV coupling parameter  $\omega = 16\mu/\kappa^2$  is introduced to control curvature square terms [25]. We note that  $\omega$  is positive and thus, a negative  $\omega$  is not allowed for the  $z = 2$  Hořava-Lifshitz gravity. In the limit of  $\omega \rightarrow \infty$  ( $\kappa^2 \rightarrow 0$ ),  $S_{\lambda=1}$  reduces to general relativity (GR) with the speed of light  $c^2 = \kappa^2\mu^3/2$  and Newton's constant  $G = \kappa^2/(32\pi c)$ . Also, we would like to mention that the last line of (2) seems to be similar to the action of 3D new massive gravity when replacing  $\mu^3$  and  $\omega$  by  $\frac{1}{16\pi cG}$  and  $m^2$ , respectively [26]. However, although a similarity between them exists, the difference is that in the  $z = 2$  Hořava-Lifshitz gravity, the curvature  $R$  is a nonrelativistic component representing the 3D space in (1+3)D spacetimes, while in the 3D new massive gravity, the 3D curvature  ${}^3R$  is a relativistic one, representing the (1+2)D spacetimes. Accordingly, the 3D new massive gravity provides higher order temporal derivatives than second order derivatives.

Let us introduce the metric for the mixmaster universe to distinguish between expansion (volume change:  $\alpha$ ) and anisotropy (shape change:  $\beta_{ij}$ )

$$ds^2 = -dt^2 + e^{2\alpha} e^{2\beta_{ij}} \sigma^i \otimes \sigma^j, \quad (3)$$

where  $\sigma^i$  are the 1 forms given by

$$\begin{aligned} \sigma^1 &= \cos \psi d\theta + \sin \psi \sin \theta d\phi, \\ \sigma^2 &= \sin \psi d\theta - \cos \psi \sin \theta d\phi, \\ \sigma^3 &= d\psi + \cos \theta d\phi \end{aligned} \quad (4)$$

on the three-sphere parameterized by Euler angles  $(\psi, \theta, \phi)$  with  $0 \leq \psi < 4\pi$ ,  $0 \leq \theta < \pi$ , and  $0 \leq \phi < 2\pi$ . The shape change  $\beta_{ij}$  is a  $3 \times 3$  traceless symmetric tensor with  $\det[e^{2\beta_{ij}}] = 1$  expressed in terms of two independent shape parameters  $\beta_{\pm}$  as

$$\beta_{11} = \beta_+ + \sqrt{3}\beta_-, \quad \beta_{22} = \beta_+ - \sqrt{3}\beta_-, \quad \beta_{33} = -2\beta_+. \quad (5)$$

The evolution of the universe is described by giving  $\beta_{\pm}$  as function of  $\alpha$ . Note that the closed FRW universe is the special case of  $\beta_{\pm} = 0$ .

Now we concentrate on the behavior near singularity. Then, the empty-space is sufficient to display the generic local evolution close to a singularity because the terms due to a matter or radiation are negligible near singularity. Using Eq. (3), the 3D curvature takes the form

$$R = -12e^{-2\alpha} V_{IR}(\beta_+, \beta_-), \quad (6)$$

where the IR-potential of curvature anisotropy is given by

$$\begin{aligned} V_{IR}(\beta_+, \beta_-) &= \frac{1}{24} \left[ 2e^{4\beta_+} \cosh(4\sqrt{3}\beta_-) + e^{-8\beta_+} \right] \\ &\quad - \frac{1}{12} \left[ 2e^{-2\beta_+} \cosh(2\sqrt{3}\beta_-) + e^{4\beta_+} \right]. \end{aligned} \quad (7)$$

The evolution of this universe is described by the motion of a point  $\beta = (\beta_+, \beta_-)$  as a function of  $\alpha$  using the time-dependent Lagrangian. The exponential wall picture of IR-potential implies that a particle (the universe) runs through almost free (Kasner) epochs where the potential could be neglected, and it is reflected at the walls, resulting infinite number of oscillations. This shows that the system under the IR-potential behaves chaotically when the singularity is approached [27].

Before we proceed, we briefly sketch the IR-potential. We mention that near the point  $(\beta_+, \beta_-) = (0, 0)$  corresponding to the global minimum, the IR-potential takes an approximate form of

$$V_{IR}(0, 0) \approx -\frac{1}{8} + (\beta_+^2 + \beta_-^2). \quad (8)$$

As is shown in Fig. 1-(a), there are three canyon lines located at  $\beta_- = 0$  and  $\beta_- = \pm\sqrt{3}\beta_+$ . We discuss the asymptotic structure of IR-potential. In the case of  $\beta_- \ll 1$ , the IR-potential is either  $V_{IR} \approx 2e^{4\beta_+}\beta_-^2$  if  $\beta_+ \rightarrow \infty$  or  $V_{IR} \approx \frac{1}{24}e^{-8\beta_+}$  if  $\beta_+ \rightarrow -\infty$ . For  $\beta_- = 0$ , one has  $V_{IR} \approx 0$  if  $\beta_+ \rightarrow \infty$ . The potential is bounded from below and exhibits discrete  $Z_3$ -symmetry by permuting the principal axes of rotation  $S^3$ . Therefore, it has the shape of an equilateral triangle in the anisotropy space  $(\beta_+, \beta_-)$  and exponentially steep walls far away from the origin. A particle can only escape to infinity along the canyon lines where the potential has the shape shown in Fig. 2 ( $\omega = 100$ ). The smallest deviation from the axial symmetry will turn the particle against the infinitely walls and thus, lead to a chaotic motion. Another useful representation of the IR-potential is shown in Fig. 3-(a) by drawing equipotential curves. They extend symmetrically between canyon lines at  $\beta_- = 0$  and  $\beta_- = \pm\sqrt{3}\beta_+$ , which correspond to a partially anisotropic universe with axial symmetry. The fully isotropic case is at the origin (0,0), where the potential takes the global minimum.

The action (2) provides the time-dependent Lagrangian

$$\begin{aligned} \mathcal{L} &= \mu^3 e^{3\alpha} \left[ -6(\dot{\alpha}^2 - \dot{\beta}_+^2 - \dot{\beta}_-^2) - 12e^{-2\alpha} V_{IR}(\beta_+, \beta_-) \right. \\ &\quad \left. + \frac{e^{-4\alpha}}{16\omega} V_{UV}(\beta_+, \beta_-) \right], \end{aligned} \quad (9)$$

where the dot denotes  $\frac{d}{cdt}$ . One needs to introduce an emergent speed of light  $c$  in order to see the UV behaviors, while for the IR behaviors, one chooses  $c = 1$  simply. Here, the UV-potential of curvature square terms takes a complicated form

$$V_{UV}(\beta_+, \beta_-) = \left[ 40 \left( e^{8\beta_+} \cosh(4\sqrt{3}\beta_-) + e^{2\beta_+} \cosh(6\sqrt{3}\beta_-) + e^{-10\beta_+} \cosh(2\sqrt{3}\beta_-) \right) - 40e^{2\beta_+} \cosh(2\sqrt{3}\beta_-) \right. \\ \left. + 4e^{-4\beta_+} \cosh(4\sqrt{3}\beta_-) + 2e^{8\beta_+} - 20e^{-4\beta_+} - 42e^{8\beta_+} \cosh(8\sqrt{3}\beta_-) - 21e^{-16\beta_+} \right], \quad (10)$$

which is a key feature of the deformed  $z = 2$  Hořava-Lifshitz gravity. Note that considering the deformed  $z = 3$  Hořava-Lifshitz gravity [11], one would expect to have a more complicated UV potential because of the presence of the Cotton tensor [28]. However, we have shown that the Cotton tensor does not change significantly the situations [29].

In order to appreciate implications of chaotic approach to the deformed  $z = 2$  Hořava-Lifshitz gravity, we have to calculate the Hamiltonian density by introducing three canonical momenta as

$$p_{\pm} = \frac{\partial \mathcal{L}}{\partial \dot{\beta}_{\pm}} = 12\mu^3 e^{3\alpha} \dot{\beta}_{\pm}, \quad p_{\alpha} = \frac{\partial \mathcal{L}}{\partial \dot{\alpha}} = -12\mu^3 e^{3\alpha} \dot{\alpha}. \quad (11)$$

The normalized canonical Hamiltonian in 6D phase space takes the form

$$\mathcal{H}_{6D} = \frac{1}{2}(p_+^2 + p_-^2 - p_{\alpha}^2) + V_{\alpha}(\beta_+, \beta_-, \omega), \quad (12)$$

where the potential is given by

$$V_{\alpha}(\beta_+, \beta_-, \omega) = e^{4\alpha} \left( V_{IR} - \frac{e^{-2\alpha}}{192\omega} V_{UV} \right). \quad (13)$$

Here  $\mathcal{H}_{6D} = 12\mu^3 e^{3\alpha} \mathcal{H}_c$  using the canonical Hamiltonian  $\mathcal{H}_c$ . In this case, let us choose the parameter  $12\mu^3 = 1$  for simplicity. Then, the Hamiltonian equations of motion are

$$\dot{\beta}_{\pm} = p_{\pm}, \quad \dot{p}_{\pm} = -e^{4\alpha} \frac{\partial V_{IR}}{\partial \beta_{\pm}} + \frac{e^{2\alpha}}{192\omega} \frac{\partial V_{UV}}{\partial \beta_{\pm}}, \\ \dot{\alpha} = -p_{\alpha}, \quad \dot{p}_{\alpha} = -4e^{4\alpha} V_{IR} + \frac{e^{2\alpha}}{96\omega} V_{UV} \quad (14)$$

in 6D phase space.

### III. CHAOTIC BEHAVIORS IN 4D PHASE SPACE

Chernoff and Barrow showed that the mixmaster 6D phase space could be split into the product of a 4D phase space showing chaotic behavior and a 2D phase space showing regular behavior [15]. Hence, we confine the dynamical system to a 4D phase space. Setting  $\alpha = 1$ , we consider the motion of a particle (the universe) of coordinates  $(\beta_+, \beta_-)$  under the full potential of

$$V_{\alpha=1}(\beta_+, \beta_-, \omega) \rightarrow V(\beta_+, \beta_-, \omega) = e^4 \left[ V_{IR} - \frac{V_{UV}}{192e^2\omega} \right]. \quad (15)$$

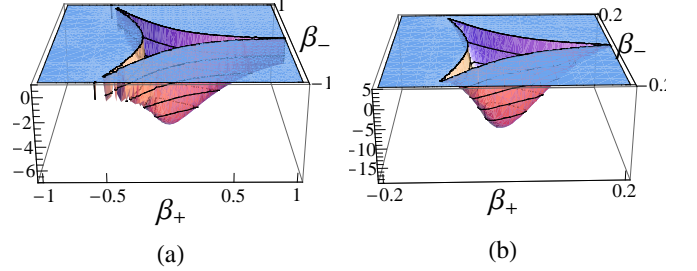


FIG. 1: 3D Potential shapes  $V(\beta_+, \beta_-, \omega)$  with three canyon lines located at  $\beta_- = 0$  and  $\beta_- = \pm\sqrt{3}\beta_+$ : (a) for  $\omega = 100$ , it corresponds to the GR mixmaster model ( $V_{IR}$  dominates). (b) For  $\omega = 0.01$ , it corresponds to the potential of  $z = 2$  Hořava-Lifshitz gravity.

The key to chaos in mixmaster dynamics is that the potential has been developed “corners”, that is, places where very special trajectories do not encounter walls. This leads to sensitive dependence on initial conditions, because a tiny change in how closely a trajectory approaches a corner can lead to large changes in the sequence of bounces off the walls. On the other hand, the behavior of the potential near the origin has little to do with chaos because the overall decrease in scale leads to the walls and the trajectories are moving ever farther outward from the origin.

Let us describe the  $z = 2$  Hořava-Lifshitz potential  $V(\beta_+, \beta_-, \omega)$  intensively. In order to make a connection to the loop quantum gravity, we first mention that near the origin  $(\beta_+, \beta_-) = (0, 0)$  which corresponds to the closed FRW universe, the potential  $V(\beta_+, \beta_-, \omega)$  takes approximately the form of

$$V(0, 0, \omega) \approx -\left(\frac{e^4}{8} + \frac{e^2}{64\omega}\right) + \left(e^4 + \frac{17e^2}{4\omega}\right)(\beta_+^2 + \beta_-^2). \quad (16)$$

Comparing (16) with (8), the former reduces to the latter up to  $e^4$  in the limit of  $\omega \rightarrow \infty$ . It turns out that adding the UV-potential makes just the potential well at the origin deeper, compared to the IR case. At this stage, it is curious to ask whether the inflection point at the origin of  $(\beta_+, \beta_-) = (0, 0)$  exists, which might show a change from chaotic behavior to non-chaotic behavior. This point may be determined by the condition of

$$V''(\beta_+, 0, \omega)|_{\beta_+=0} = V''(0, \beta_-, \omega)|_{\beta_-=0} = 0, \quad (17)$$

which leads to

$$2e^4 + \frac{17e^2}{2\omega} = 0. \quad (18)$$

However, we have the negative  $\omega_c$

$$\omega_c = -\frac{17}{4e^2} \simeq -0.5752. \quad (19)$$

This may imply that there is no inflection point which makes a transition from chaotic behavior to non-chaotic behavior.

The asymptotic structure of the full potential is given as follows. For  $\beta_- = 0$ , if  $\beta_+ \rightarrow \infty$ , then

$$V(\beta_+, \beta_-, \omega) \approx 0. \quad (20)$$

For  $\beta_- \ll 1$ , if  $\beta_+ \rightarrow \infty$ , one finds

$$e^{-2}V(\beta_+, \beta_-, \omega) \approx \frac{16\beta_-^2}{\omega} e^{8\beta_+}. \quad (21)$$

For  $\beta_- \ll 1$ , if  $\beta_+ \rightarrow -\infty$ , then

$$e^{-2}V(\beta_+, \beta_-, \omega) \approx \frac{7}{64\omega} e^{-16\beta_+}. \quad (22)$$

Therefore, the asymptotic structure is determined by the UV-potential. As is shown in Fig. 1-(b), there are three canyon lines located at  $\beta_- = 0$  and  $\beta_- = \pm\sqrt{3}\beta_+$ . The potential is bounded from below and exhibits discrete  $Z_3$ -symmetry by permuting the principal axes of rotation  $S^3$ . Therefore, it has the shape of an equilateral triangle in the anisotropy space  $(\beta_+, \beta_-)$  and exponentially steep walls far away from the origin. However, for total energy  $E < V_{lm}$ , a particle cannot escape to infinity along the canyon lines where the potential has a local maximum  $V = V_{lm}$  as a bump shown in Fig. 2 ( $\omega = 0.01$ ). For  $E < 0$ , the smallest deviation from the axial symmetry will turn the particle against the infinitely walls and thus, lead to a chaotic motion. Although a local maximum appears along canyon lines, equipotential curves in Fig. 3-(b) are similar to Fig. 3-(a) of IR-potential for  $E < 0$ . Hence, we expect that chaotic behavior appears in the  $z = 2$  Hořava-Lifshitz gravity with small  $\omega$ . The

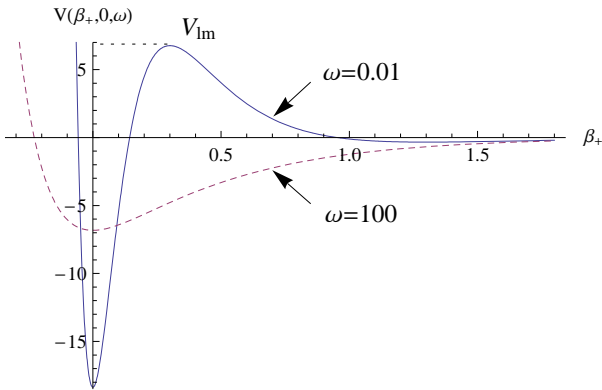


FIG. 2: Potential graphs  $V(\beta_+, \beta_-, \omega)$  with  $\beta_- = 0$ : the long-dashed curve is for  $\omega = 100$  (GR) and the solid curve for  $\omega = 0.01$  with a local maximum  $V = V_{lm}$ .

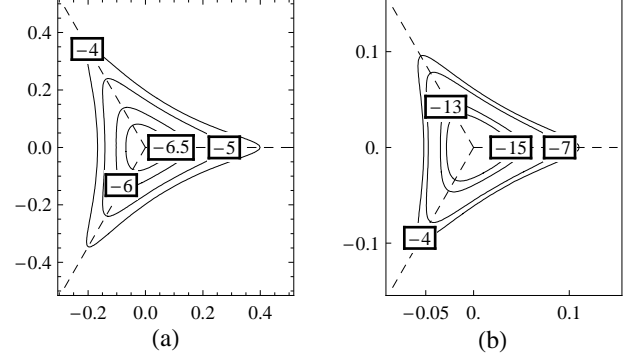


FIG. 3: Equipotential curves, developing triangles with corner: (a) for  $\omega = 100$  with  $E = -6.5, -6.0, -5.0, -4.0$ , respectively, (b) for  $\omega = 0.01$  with  $E = -15.0, -13.0, -7.0, -4.0$ , respectively. Three canyon lines are developed along corners at  $\beta_- = 0$  and  $\beta_- = \pm\sqrt{3}\beta_+$ .

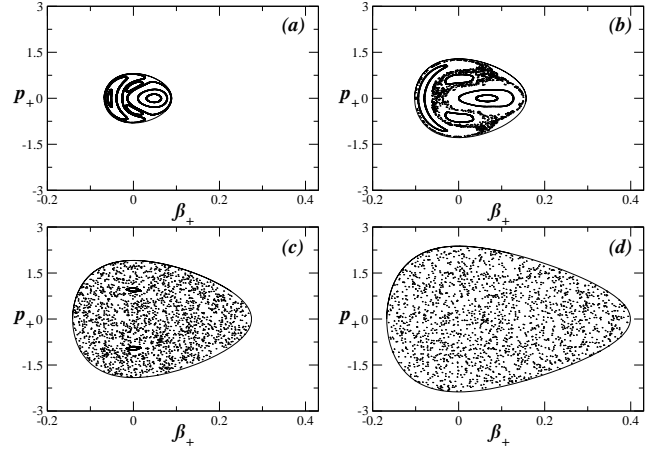


FIG. 4: Poincaré sections for the  $\omega = 100$  case with (a)  $E = -6.5$ , (b)  $E = -6.0$ , (c)  $E = -5.0$ , and (d)  $E = -4.0$ .

dynamics of particle seems complicated for  $0 < E < V_{lm}$  and thus, we skip it.

In general, the chaos could be defined as being such that (i) the periodic points of the flow associated to the Hamiltonian are dense, (ii) there is a transitive orbit in the dynamical system, and (iii) there is sensitive dependence on the initial condition. Our reduced system is described by the 4D Hamiltonian

$$\mathcal{H}_{4D} = \frac{1}{2}(p_+^2 + p_-^2) + V(\beta_+, \beta_-, \omega). \quad (23)$$

It is well known that the appearance of chaotic behavior in the mixmaster dynamics is closely related to the appearance of “corner” potential. To make a definite connection, we choose  $\omega = 100$  and  $\omega = 0.01$  for the original mixmaster universe of GR and the mixmaster universe of  $z = 2$  Hořava-Lifshitz gravity, respectively. As is shown in Fig. 3, when making equipotential curves, we find that the corner appears for  $E = -5.0$  and  $-4.0$  for  $\omega = 100$

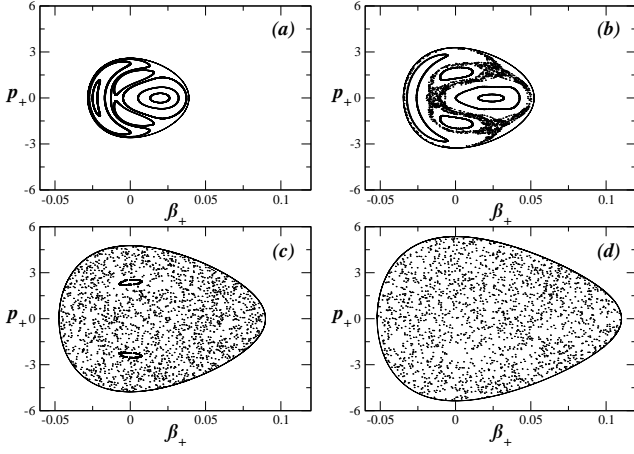


FIG. 5: Poincaré sections for  $\omega = 0.01$  with (a)  $E = -15.0$ , (b)  $E = -13.0$ , (c)  $E = -7.0$ , and (d)  $E = -4.0$ .

and for  $E = -7.0$  and  $-4.0$  for  $\omega = 0.01$ , which implies the appearance of chaos.

Let us perform simulations of the 4D dynamics and represent Poincaré sections, which describe the trajectories in phase space  $(p_+, \beta_+)$  by varying the total energy  $E$  or  $\mathcal{H}_{4D}$  of the system. Actually, we have performed the analysis for the  $\omega = 100, 1, 0.03$ , and  $0.01$  cases. We have found that the chaotic behavior persists for all  $\omega > 0$ . Figs. 4 and 5 present two typical cases, showing that the intersections of several computed trajectories are displaced in  $(p_+, \beta_+)$  with the plane  $\beta_- = 0$  for different values of energies. In each plot, we choose initial points which correspond to a prescribed kinetic energy. Also we confirm that for  $\omega = 0.01$ , complicated chaotic behaviors appear for  $0 < E < V_{lm}$ .

The results of Poincaré sections show that considering lower energies  $E = -6.5$  and  $-6.0$  for  $\omega = 100$  and  $E = -15.0$  and  $-13.0$  for  $\omega = 0.01$  within the potential well, the integrable behavior dominates and the intersections of trajectories represent closed curves. Importantly, concerning higher energies  $E = -5.0$  and  $-4.0$  for  $\omega = 100$  and  $E = -7.0$  and  $-4.0$  for  $\omega = 0.01$  within the potential well, *the closed curves are broken up gradually and the bounded phase space fills with a chaotic sea*. The same kinds of plots have been obtained for the other phase space  $(p_-, \beta_-)$  with the plane  $\beta_+ = 0$ . At this stage, we mention that for  $\omega = 100$ , the case of  $E = 0$  leads to the “corners”, where special trajectories do not encounter walls. However, for  $\omega = 0.01$ , the case of  $E = 0$  does not lead to the “corner” because of the presence of a local maximum. For this, see Fig. 2.

Finally, it confirms that the appearance of chaotic behavior in the mixmaster dynamics of  $z = 2$  Hořava-Lifshitz gravity is closely related to the appearance of corner.

#### IV. CHAOTIC BEHAVIOR IN 6D PHASE SPACE

Up to now, we have investigated the dynamics at fixed  $\alpha = 1$  for simplicity. This means that we have never explored the outer region of the potential which also determines whether the  $z = 2$  Hořava-Lifshitz gravity is chaotic. We remind the reader that the true phase space is 6D for the vacuum universe, and thus, we have to consider a movable billiard with the potential  $V_\alpha(\beta_+, \beta_-, \omega)$  in Eq. (13) because the walls are moving with time since the logarithm of the volume change  $\alpha = \frac{1}{3} \ln V$  and its derivative are entering in the system. In this case,  $\alpha$  and  $p_\alpha$  are regular variables as functions of time. Therefore, one should perform a full simulation which includes the dynamics of  $\alpha$  and  $p_\alpha$ . However, this seems to be a formidable task and thus, we could not make a progress on this direction.

In this section, instead, we will investigate a possibility of finding chaotic behaviors by considering the small volume limit of  $\alpha \rightarrow -\infty$  only. To this end, it would be better to introduce a new time  $\tau$  defined by

$$\tau = \int \frac{dt}{V}, \quad V = e^{3\alpha}, \quad (24)$$

which makes decoupling of the volume  $\alpha$  from the shape  $\beta_\pm$  explicitly. Starting from the action (2) and integrating out the space variables, we have

$$\begin{aligned} \bar{S}_{\lambda=1} = & \mu^3 \int d\tau \frac{e^{3\alpha} N}{V} \left[ 6(-\alpha'^2 + \beta_+^{\prime 2} + \beta_-^{\prime 2}) \right. \\ & \left. - V^2 \left( 12e^{-2\alpha} V_{IR}(\beta_+, \beta_-) - \frac{e^{-4\alpha}}{16\omega} V_{UV}(\beta_+, \beta_-) \right) \right], \end{aligned} \quad (25)$$

where the prime ( $'$ ) denotes the derivatives with respect to  $\tau$ . Plugging  $N = 1$  into (25), we have the Lagrangian as

$$\begin{aligned} \bar{\mathcal{L}}_{\lambda=1} = & \mu^3 \left[ 6(-\alpha'^2 + \beta_+^{\prime 2} + \beta_-^{\prime 2}) \right. \\ & \left. - 12e^{4\alpha} \left( V_{IR}(\beta_+, \beta_-) - \frac{e^{-2\alpha}}{192\omega} V_{UV}(\beta_+, \beta_-) \right) \right]. \end{aligned} \quad (26)$$

The canonical momenta are given by

$$\bar{p}_\pm = \frac{\partial \bar{\mathcal{L}}_{\lambda=1}}{\partial \beta'_\pm} = 12\mu^3 \beta'_\pm, \quad \bar{p}_\alpha = \frac{\partial \bar{\mathcal{L}}_{\lambda=1}}{\partial \alpha'} = -12\mu^3 \alpha'. \quad (27)$$

Then, the canonical Hamiltonian in 6D phase space is obtained to be

$$\begin{aligned} \bar{\mathcal{H}}_{6D} = & \bar{p}_\alpha \alpha' + \bar{p}_+ \beta'_+ + \bar{p}_- \beta'_- - \bar{\mathcal{L}}_{\lambda=1} \\ = & \frac{1}{2}(\bar{p}_+^2 + \bar{p}_-^2 - \bar{p}_\alpha^2) + e^{4\alpha} \left( V_{IR} - \frac{e^{-2\alpha}}{192\omega} V_{UV} \right), \end{aligned} \quad (28)$$

where we have chosen the parameter  $12\mu^3 = 1$  for simplicity. Then, the Hamiltonian equations of motion are obtained as

$$\begin{aligned}\beta'_\pm &= \bar{p}_\pm, \quad \bar{p}'_\pm = -e^{4\alpha} \frac{\partial V_{IR}}{\partial \beta_\pm} + \frac{e^{2\alpha}}{192\omega} \frac{\partial V_{UV}}{\partial \beta_\pm}, \\ \alpha' &= -\bar{p}_\alpha, \quad \bar{p}'_\alpha = -4e^{4\alpha} V_{IR} + \frac{e^{2\alpha}}{96\omega} V_{UV}.\end{aligned}\quad (29)$$

We note that comparing Eqs. (29) with Eqs. (14), there is no change in the Hamiltonian and its equations of motion except replacing  $t$  by  $\tau$ . The evolution of  $\alpha$  is in particular determined by

$$\alpha'' = 4e^{4\alpha} V_{IR} - \frac{e^{2\alpha}}{96\omega} V_{UV}. \quad (30)$$

Then, we obtain a 6D phase space consisting in the product of a 4D chaotic one times a 2D regular phase space for the  $\alpha$  and  $p_\alpha$  variables. As the volume goes to zero near singularity ( $e^{4\alpha} \rightarrow 0$ ,  $p_\alpha \rightarrow 0$ ), one finds the limit

$$\bar{\mathcal{H}}_{6D} \rightarrow \frac{1}{2}(\bar{p}_+^2 + \bar{p}_-^2) + K \neq \mathcal{H}_{4D}. \quad (31)$$

Hence, we note that the 6D system is not asymptotic in  $\tau$  to the previous 4D system.

Now, we are in a position to show that the presence of the UV-potential does not suppress chaotic behaviors existing in the IR-potential. For this purpose, we have to introduce two velocities: particle velocity  $v_p$  and wall velocity  $v_w$  defined by

$$v_p = \sqrt{\bar{p}_+^2 + \bar{p}_-^2}, \quad v_w = \frac{d\beta_+^w}{d\tau}, \quad (32)$$

where the wall location  $\beta_+^w$  is determined by the fact that the asymptotic potential  $K$  is significantly felt by the particle as

$$\bar{p}_\alpha^2 \approx 2K = \frac{e^{4\alpha-8\beta_+}}{12} + \frac{7e^{2\alpha-16\beta_+}}{32\omega} \quad (33)$$

in the limit of  $\beta_+ \rightarrow -\infty$ . On the other hand, the particle velocity is given by

$$v_p = \sqrt{2\bar{\mathcal{H}}_{6D} + \bar{p}_\alpha^2 - 2K}. \quad (34)$$

In the IR-limit ( $\omega \rightarrow \infty$ ) of Einstein gravity, the wall location is determined by

$$\beta_+^w \approx \frac{\alpha}{2} - \frac{1}{8} \ln [12\bar{p}_\alpha^2]. \quad (35)$$

Then, the wall velocity is given by

$$v_w^{IR} = -\frac{d\beta_+^w}{d\tau} \approx \frac{\bar{p}_\alpha}{2} + \frac{e^{4\alpha-8\beta_+}}{24\bar{p}_\alpha}, \quad (36)$$

which leads to

$$|v_w^{IR}| \approx \frac{|\bar{p}_\alpha|}{2}. \quad (37)$$

As a result, we find that the particle velocity is always greater than the wall velocity as

$$v_p^{IR} = \sqrt{2\bar{\mathcal{H}}_{6D} + \bar{p}_\alpha^2 - 2e^{4\alpha} V_{IR}} \approx |\bar{p}_\alpha| > v_w^{IR}. \quad (38)$$

Thus, there will be an infinite number of collisions of the particle against the wall since it will always catch a wall [19, 20].

Next, let us investigate what happens in the UV-limit of  $\omega \rightarrow 0$ . In this case, the  $V_{UV}$  term dominates. The wall velocity takes the form

$$|v_w^{UV}| = \frac{|\bar{p}_\alpha|}{8}, \quad (39)$$

and the particle velocity leads to

$$v_p^{UV} \approx |\bar{p}_\alpha| > |v_w^{UV}| \quad (40)$$

in the limit of  $\alpha \rightarrow -\infty$ . This case is similar to the Einstein gravity.

Finally, we could not observe a slowing down of the particle velocity due to the UV effects. This means that the chaos persists in the moving wall.

## V. DISCUSSIONS

First of all, we point out that for  $\omega > 0$ , there always exists chaotic behavior. This contrasts to the case of the loop mixmaster dynamics based on loop quantum cosmology [23], where the mixmaster chaos could be suppressed by loop quantum effects [22]. In the loop quantum cosmology, the effective potential at decreasing volume labeled by “discreteness  $j$ ” are significantly changed in the vicinity of (0,0)-isotropy point in the anisotropy plane  $-\beta_+$ . The potential at larger volumes exhibits a potential wall of finite height and finite extension like Fig. 2. As the volume is decreased, the wall moves inward and its height decreases. Progressively, the wall disappears completely making the potential negative everywhere at a dimensionless volume of  $(2.172j)^{3/2}$  in the Planck units. Eventually, the potential approach zero from below. This shows that classical reflections will stop after a finite amount of time, implying that classical arguments about chaos inapplicable. Once quantum effects are taken into account, the reflections stop just when the volume of a given patch is about the size of Planck volume.

To that end, the role of UV coupling parameter  $\omega$  is different from the area quantum number  $j$  of the loop quantum gravity. In our case, time variable (related to the volume of  $V = e^{3\alpha}$ ) as well as two physical degrees of anisotropy  $\beta_\pm$  are treated in the classical way without quantization. However, in the loop quantum framework, all three scale factors were quantized using the loop techniques. Hence two are quite different: the potential wells at the origin did not disappear for any  $\omega > 0$  in the  $z = 2$  Hořava-Lifshitz gravity, while in the loop quantum

gravity the height of potential wall rapidly decreases until they disappears completely as the Planck scale is reached.

At this stage, we compare our results with the mixmaster universe in the generalized uncertainty principle (GUP) [31]. Considering a close connection between  $z = 2$  Hořava-Lifshitz gravity and GUP [25], there may exist a cosmological relation between them. Fortunately, the chaotic behavior of the Bianchi IX model was not tamed by GUP effects, which means that the deformed mixmaster universe is still a chaotic system. This is mainly because two physical degrees of anisotropy  $\beta_{\pm}$  are considered as deformed while the time variable is treated in the classical way. This supports that our approach without quantization is correct.

Furthermore, it was shown that adding  $({}^4R)^2$  (and possibly other) curvature terms to the general relativity leads to the fact that the chaotic behavior is absent [32]. Hence it is very curious to see why  $({}^4R)^2$  does suppress chaotic behavior, but  $-\frac{2}{\omega}(R_{ij}R^{ij} - \frac{3}{8}R^2)$  does not suppress chaotic behavior.

In conclusion, the mixmaster universe has provided another example that  $z = 2$  Hořava-Lifshitz gravity has shown chaotic behavior, as other chaotic dynamics of string or M-theory cosmology models [30]. This may be because we did not quantize the Hořava-Lifshitz gravity and we did study its classical aspects.

## Acknowledgments

Y.S. Myung and Y.-W. Kim were supported by Basic Science Research Program through the National Research Foundation (NRF) of Korea funded by the Ministry of Education, Science and Technology (2009-0086861). W.-S. Son and Y.-J. Park were supported by the Korea Science and Engineering Foundation (KOSEF) grant funded by the Korea government (MEST) through WCU Program (No. R31-20002).

- 
- [1] P. Horava, JHEP **0903**, 020 (2009) [arXiv:0812.4287 [hep-th]].
  - [2] P. Horava, Phys. Rev. D **79**, 084008 (2009) [arXiv:0901.3775 [hep-th]].
  - [3] P. Horava, Phys. Rev. Lett. **102**, 161301 (2009) [arXiv:0902.3657 [hep-th]].
  - [4] G. Calcagni, JHEP **0909**, 112 (2009) [arXiv:0904.0829 [hep-th]].
  - [5] E. Kiritsis and G. Kofinas, Nucl. Phys. B **821**, 467 (2009) [arXiv:0904.1334 [hep-th]].
  - [6] S. Mukohyama, JCAP **0906**, 001 (2009) [arXiv:0904.2190 [hep-th]].
  - [7] T. Takahashi and J. Soda, Phys. Rev. Lett. **102**, 231301 (2009) [arXiv:0904.0554 [hep-th]].
  - [8] R. Brandenberger, Phys. Rev. D **80**, 043516 (2009) [arXiv:0904.2835 [hep-th]].
  - [9] S. Kalyana Rama, Phys. Rev. D **79**, 124031 (2009) [arXiv:0905.0700 [hep-th]].
  - [10] G. Leon and E. N. Saridakis, JCAP **0911**, 006 (2009) [arXiv:0909.3571 [hep-th]].
  - [11] A. Kehagias and K. Sfetsos, Phys. Lett. B **678**, 123 (2009) [arXiv:0905.0477 [hep-th]].
  - [12] Y. S. Myung, Phys. Lett. B **678**, 127 (2009) [arXiv:0905.0957 [hep-th]].
  - [13] C. W. Misner, Phys. Rev. Lett. **22**, 1071 (1969).
  - [14] B. L. Hu and T. Regge, Phys. Rev. Lett. **29**, 1616 (1972).
  - [15] D. F. Chernoff and J. D. Barrow, Phys. Rev. Lett. **50**, 134 (1983).
  - [16] N. J. Cornish and J. J. Levin, Phys. Rev. Lett. **78**, 998 (1997) [arXiv:gr-qc/9605029].
  - [17] N. J. Cornish and J. J. Levin, Phys. Rev. D **55**, 7489 (1997) [arXiv:gr-qc/9612066].
  - [18] M. P. Dabrowski, Phys. Lett. B **474**, 52 (2000) [Phys. Lett. B **496**, 226 (2000)] [arXiv:hep-th/9911217].
  - [19] T. Lehner and L. Di Menza, Chaos Solitons Fractals **16**, 597 (2003).
  - [20] L. Di Menza and T. Lehner, Gen. Rel. Grav. **36**, 2635 (2004).
  - [21] V. A. Belinsky, I. M. Khalatnikov and E. M. Lifshitz, Adv. Phys. **19**, 525 (1970).
  - [22] M. Bojowald and G. Date, Phys. Rev. Lett. **92**, 071302 (2004) [arXiv:gr-qc/0311003].
  - [23] M. Bojowald, Living Rev. Rel. **8**, 11 (2005) [arXiv:gr-qc/0601085].
  - [24] R.L. Arnowitt, S. Deser and C.W. Misner, *The dynamics of general relativity*, "Gravitation: an introduction to current research", Louis Witten ed. (Wiley 1962), chapter 7, pp 227-265, arXiv:gr-qc/0405109.
  - [25] Y. S. Myung, Phys. Lett. B **684**, 1 (2010) [arXiv:0911.0724 [hep-th]].
  - [26] E. A. Bergshoeff, O. Hohm and P. K. Townsend, Phys. Rev. Lett. **102**, 201301 (2009) [arXiv:0901.1766 [hep-th]].
  - [27] T. Damour, M. Henneaux and H. Nicolai, Class. Quant. Grav. **20**, R145 (2003) [arXiv:hep-th/0212256].
  - [28] I. Bakas, F. Bourliot, D. Lust and M. Petropoulos, Class. Quant. Grav. **27**, 045013 (2010) [arXiv:0911.2665 [hep-th]].
  - [29] Y. S. Myung, Y. W. Kim, W. S. Son and Y. J. Park, JHEP **1003**, 085 (2010) [arXiv:1001.3921 [gr-qc]].
  - [30] T. Damour and M. Henneaux, Phys. Rev. Lett. **85**, 920 (2000) [arXiv:hep-th/0003139].
  - [31] M. V. Battisti and G. Montani, Phys. Lett. B **681**, 179 (2009) [arXiv:0808.0831 [gr-qc]].
  - [32] J. D. Barrow and H. Sirousse-Zia, Phys. Rev. D **39**, 2187 (1989); J. D. Barrow and S. Cotsakis, Phys. Lett. B **232**, 172 (1989); S. Cotsakis, J. Demaret, Y. de Rop and L. Querella, Phys. Rev. D **48**, 4595 (1993).